

Daytime E-Region Irregularities During the 22 July 2009 Solar Eclipse over Chung-Li (24.9°N, 121.2°E), a Moderate Mid-Latitude Station

Potula Sree Brahmanandam*, Yen Hsyang Chu, Ching-Lun Su, and Ting-Han Lin

Institute of Space Science, National Central University, Chung-Li, Taiwan

Received 9 May 2013, accepted 8 July 2013

ABSTRACT

The 22 July 2009 solar eclipse with an obscuration of > 83% at Chung-Li (24.9°N, 121.2°E, Dip 35°N) in Taiwan during noon hours has provided a unique opportunity for us to examine its impact on E-region irregularities which were observed simultaneously by the 52 MHz coherent radar and a co-located ionosonde. Significant observations revealed that the daytime E-region strong backscatter echoes at multiple heights and a sudden intensification of the weak sporadic E-layer during the 22 July 2009 solar eclipse. These results follow the research findings of Patra et al. (2009). As the incident solar radiation suddenly blocked by intruding Moon during solar eclipse events that would generally create night-like ionospheric conditions, it is surmised that the E-region irregularities were indeed induced by the eclipse associated effects. The induced effects resulted in faster recombination of molecular ions, generation of gravity waves and electric fields that could have created a conducive environment to excite plasma irregularities through a gradient-drift instability mechanism. The vertical shears of radar Doppler velocity and the peak radar backscatter at the node of Doppler velocity shear, as resolved by the coherent scatter radar with interferometer technique, were possibly due to the upward propagating gravity waves and wave-induced polarization electric fields. The present observational results should not only be highly useful to ascertain plausible mechanisms responsible for nighttime E-region irregularities, but also provided evidence that a solar eclipse could generate E-region plasma irregularities over temperate mid-latitudes for the first time.

Key words: Solar eclipse, Ionospheric irregularities, Mid-latitude ionosphere, Wave propagation

Citation: Brahmanandam, P. S., Y. H. Chu, C. L. Su, and T. H. Lin, 2013: Daytime E-region irregularities during the 22 July 2009 solar eclipse over Chung-Li (24.9°N, 121.2°E), a moderate mid-latitude station. *Terr. Atmos. Ocean. Sci.*, 24, 1021-1032, doi: 10.3319/TAO.2013.07.08.01(AA)

1. INTRODUCTION

Observing a solar eclipse provides a unique opportunity to study various atmospheric processes as it temporarily cuts off solar radiation which is responsible for almost all the physical mechanisms occurring within the Earth's atmosphere. During an eclipse epoch, usual processes of production and ionospheric loss are disturbed locally for a brief period (for example, Van Zandt et al. 1960; West et al. 2008). Because the formation mechanisms of lower ionospheric layers (E and F1) are dictated predominantly by the amount of solar radiation, which is otherwise absent during solar eclipses, a substantial decay in the plasma densities of E and F1 layers is inevitable (for example, Van Zandt et al. 1960; Davies et al. 1964; Tsai and Liu 1997; Le et al. 2008).

In addition, a few recent studies have provided evi-

dence that a solar eclipse can induce/enhance plasma irregularities in the E-region (Sridharan et al. 2002; Patra et al. 2009; Thampi et al. 2010). For example, Sridharan et al. (2002) used both HF and VHF radar observations from Trivandrum (8.5°N, 77°E, Dip 0.5°N), a typical equatorial station in India, to investigate the exact effects of electrodynamics on the equatorial E and F-regions during a partial solar eclipse that passed over Trivandrum during pre-sunset hours on 11 August 1999; a few unique features were observed including the sudden intensification of a weak blanketing sporadic E-layer (Es layer) and the associated large enhancement of the VHF backscattered returns, significant increase in h'F (base height of F layer) and distinctly different spatial and temporal structures in spread-F irregularity drift velocities. Though Sridharan et al. (2002) merely linked the phenomenon of sudden intensification of a weak blanketing Es layer to the solar eclipse induced effects, they

* Corresponding author
E-mail: anandp@jupiter.ss.ncu.edu.tw

interpreted the significant height rise in $h'F$ in terms of a local enhancement in the F-region electric field resulting from a plasma density reduction in the low latitude E-region that is electro-dynamically connected to the equatorial F-region through geomagnetic field lines.

Away from equatorial regions, Patra et al. (2009) and Thampi et al. (2010) used VHF radars located at Gadanki (13.5°N, 79.2°E, Dip 12.5°N), a low-latitude station in India, and at Shigaraki (35.85°N, 136.1°E, Dip 48°N), a mid-latitude station in Japan, to investigate local E-region responses to solar eclipses; both stations have observed E-region plasma density irregularities during partial solar eclipses which occurred on 11 August 1999 and 22 July 2009, respectively. Both Patra et al. (2009) and Thampi et al. (2010) hypothesized that a solar eclipse could provide 'night-like' conditions which allow the excitation of plasma instability and the generation of plasma irregularities. Further, they conjectured that the irregularities could grow on density gradients formed by the metallic ion layers when molecular ions were recombined during solar eclipse events, although they did not mention the causative mechanism responsible for the formation of metallic ion layers. Also, recently Patra et al. (2011) found 150 km daytime irregularities, so-called valley region irregularities using the Gadanki VHF radar during 15 January 2010 solar eclipse. In this context, to ascertain that the E-region irregularities were indeed induced by a solar eclipse and not a chance occurrence or had occurred due to the availability of other free energy sources responsible for daytime irregularities as reported by Patra et al. (2009), observational studies on these rare and unique natural events along the path of eclipse are very much needed, and these aspects ignite us to carry-out the present research. Further, it would be most interesting to investigate whether daytime E-region irregularities are observed (or not) during the longest solar eclipse which occurred on 22 July 2009 over a typical equatorial ionization anomaly crest zone station such as Chung-Li (Geographic Lat. 24.9°N, Geographic Long. 121.2°E, Dip 35°N) which is located at temperate mid-latitudes exactly in between the Gadanki and Shigaraki latitudes and where the nighttime backscatter echoes using the 52 MHz radar have been long reported (Chu et al. 1996; Chu and Wang 1997). By doing so, it may be possible to certify whether a solar eclipse could really induce plasma irregularities in the E-region over low and mid-latitudes or such irregularities belong to the category of mere daytime E-region irregularities observed over Gadanki (Patra et al. 2004, 2006). In addition, the present observations should be useful to know the exact mechanisms responsible for nighttime E-region irregularities over moderate mid latitudes.

Further, the recent studies associated with the 22 July 2009 solar eclipse have reported clear evidence on eclipse induced effects on both the lower (Chen et al. 2010) and upper ionosphere (Liu et al. 2011). Importantly, Liu et al. (2011) found bow and stern waves, which are formed by

acoustic gravity waves, in total electron content (TEC) measured using a dense ground-based GPS receiver network over Taiwan during the passage of Moon's shadow boat (the cooling region). Liu et al. (2011) research has provided evidence on the presence of gravity waves during the present solar eclipse epoch over Taiwan and that a gravity wave could have helped in the formation of a Es layer (Hines 1960; Datta 1972).

We operated the 52 MHz Chung-Li VHF radar along with a co-located ionosonde radar to study the E-region irregularities during the partial solar eclipse which occurred on 22 July 2009. Most importantly, for the first time the measurements of vertical shear of 3-m FAI Doppler velocity in moderate middle latitude Es regions have been made by coherent radar with the interferometer technique during a solar eclipse. Several important features were observed including quasi-periodic (QP) type echoes for about 45 minutes from 0935 to 1020 LT (LT = UT + 0800 hours) and for about 55 minutes from 1040 to 1135 LT when a sudden and intensified Es layer appeared during above periods. In addition, multiple layers were observed, albeit for a short time, by both VHF and ionosonde radars during the peak time of solar eclipse. Daytime QP echoes were observed over this location for the first time during a solar eclipse event. With this concrete observational evidence, it may be reasonable to conclude that the solar eclipses are able to induce plasma irregularities in the E-region over low and mid-latitudes during daytime hours.

This article is organized as follows: section 2 contains typical observational results. Discussion on the possible generation mechanism of E-region irregularities during daytime when the longest solar eclipse passing with supersonic speeds over the Taiwan region is given in section 3 and finally, a summary and conclusion are provided in section 4.

2. OBSERVATIONS

The longest total solar eclipse over the next hundred years occurred on 22 July 2009 and swept over the East Asian region during a noontime period. Figure 1 depicts the path of the eclipse, which is provided courtesy of F. Espenak of NASA (<http://eclipse.gsfc.nasa.gov/SEplot/SEplot2001/SE2009Jul22T.GIF>). This is the standard format for eclipse plots on the NASA site and contains ephemeris and geocentric libration (West et al. 2008). As it is evident from Fig. 1, the path of the lunar umbra shadow commenced initially in India and crossed over Nepal, Bangladesh, Bhutan, Myanmar, and China. The point of greatest eclipse occurred over the western Pacific Ocean region, which is about 100 km south of the Bonin Islands located near the south east of Japan.

The 22 July 2009 solar eclipse was a partial solar eclipse over the Taiwan region and over the present radar beam location an 83% obscuration occurred. The event occurred within the interval of 0823 - 1105 LT (LT = UT + 0800 hours) with

Total Solar Eclipse of 2009 Jul 22

Geocentric Conjunction = 02:33:04.4 UT J.D. = 2455034.606301

Greatest Eclipse = 02:35:21.1 UT J.D. = 2455034.607884

Eclipse Magnitude = 1.0799 Gamma = 0.0696

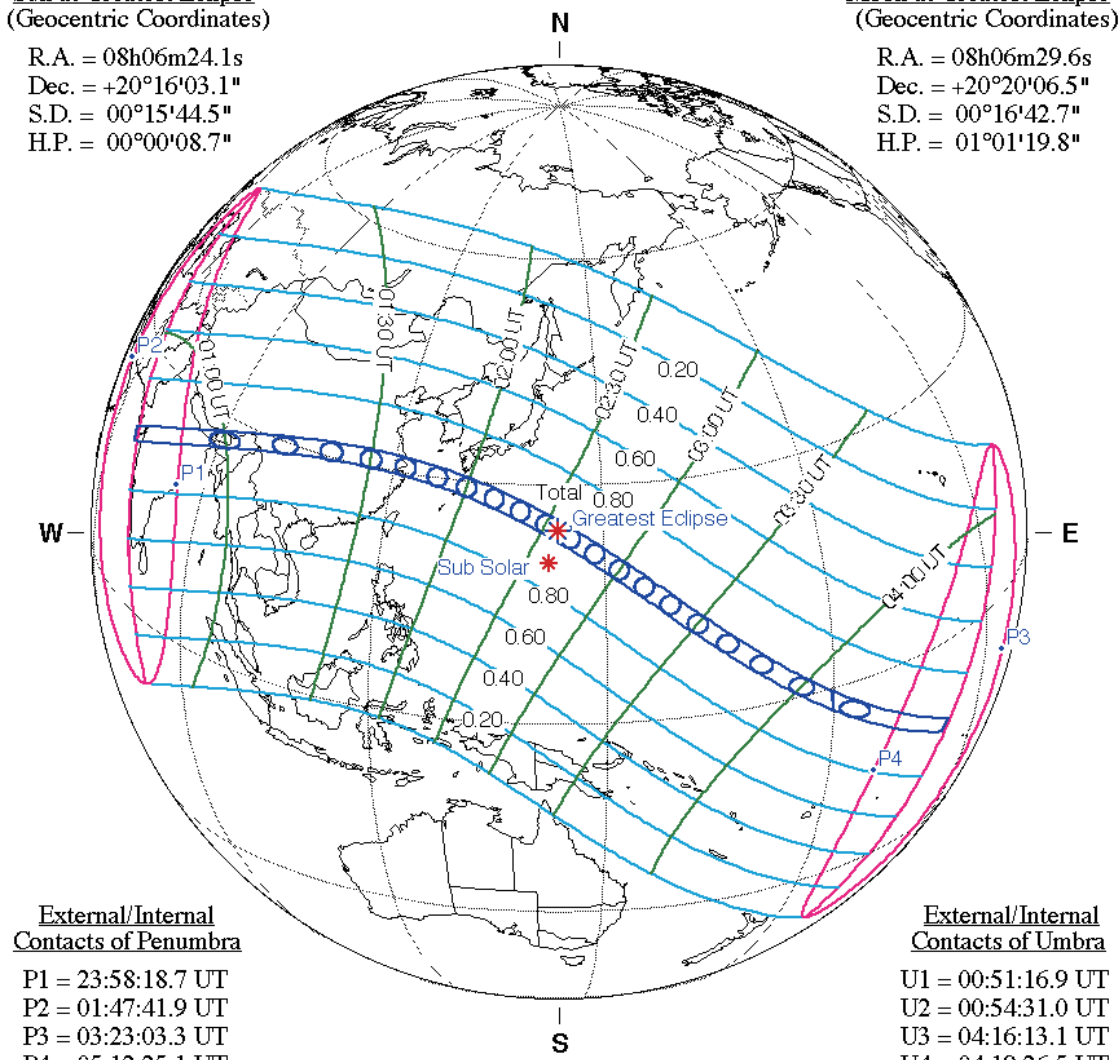
Saros Series = 136 Member = 37 of 71

Sun at Greatest Eclipse
(Geocentric Coordinates)

R.A. = 08h06m24.1s
Dec. = +20°16'03.1"
S.D. = 00°15'44.5"
H.P. = 00°00'08.7"

Moon at Greatest Eclipse
(Geocentric Coordinates)

R.A. = 08h06m29.6s
Dec. = +20°20'06.5"
S.D. = 00°16'42.7"
H.P. = 01°01'19.8"



External/Internal Contacts of Penumbra

P1 = 23:58:18.7 UT
P2 = 01:47:41.9 UT
P3 = 03:23:03.3 UT
P4 = 05:12:25.1 UT

External/Internal Contacts of Umbra

U1 = 00:51:16.9 UT
U2 = 00:54:31.0 UT
U3 = 04:16:13.1 UT
U4 = 04:19:26.5 UT

Local Circumstances at Greatest Eclipse

Lat. = 24°12.6'N Sun Alt. = 85.9°
Long. = 144°06.4'E Sun Azm. = 197.6°
Path Width = 258.4 km Duration = 06m38.8s

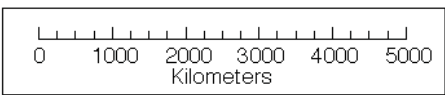
Ephemeris & Constants

Eph. = Newcomb/ILE
 $\Delta T = 66.2$ s
k1 = 0.2724880
k2 = 0.2722810
 $\Delta b = 0.0''$ $\Delta l = 0.0''$

Geocentric Libration
(Optical + Physical)

l = 0.66°
b = -0.09°
c = 10.53°

Brown Lun. No. = 1071



F. Espenak, NASA's GSFC - Fri, Jul 2,
sunearth.gsfc.nasa.gov/eclipse/eclipse.html

Fig. 1. Extent of the total solar eclipse of 22 July 2009, showing the complete path as well as lines of percentage occultation of the solar disk and declination of the leading edge of the eclipse (Courtesy of F. Espenak of NASA, 2004).

maximum obscuration at 0940 LT. The pertinent times of initial, maximum, and ending phases of this solar eclipse are indicated by vertical lines in green in Figs. 2, 3 and 4. Both VHF radar and ionosonde were operated one week before and after the eclipse event day to study the effect of solar eclipse on E-region plasma processes. Nevertheless, we show here only the observations results during 21 (pre-eclipse day) and 22 July 2009 (during eclipse day). The 52 MHz radar observations were performed in interferometry mode (Chu and Wang 1997) and the true heights of backscatter echoes in this present study were determined with interferometry analysis, not with the conventional method (i.e., $h = r \times \sin(\theta)$, where 'r' is the range and θ is the direction of perpendicularity to the magnetic field lines) with which only apparent or approximate height can be determined (Wang and Chu 2001). On the other hand, the ionosonde was used cyclically at 5 minute intervals to provide ionograms. The configuration of radar experiment along with important parameters used for the present study is given in Table 1.

The top, middle and lower panels in Fig. 2 show the Range-Time-Intensity (RTI) map along with Doppler velocities and spectral widths of the echoes observed on 21 July 2009. As is shown, no predominant backscatter echoes were present, although strong backscatter echoes were present during post-sunset hours (not shown). The middle panel in Fig. 2 shows the Doppler velocities for the radar data taken in the above period, in which the positive (negative) Doppler velocity represents the target moving away (approaching toward)

the radar. Figure 3 shows the RTI map, Doppler velocities and spectral widths of backscatter echoes observed on 22 July 2009. The RTI plots display echoes from the E-region field-aligned irregularities (FAIs), with the presence of typical morning time "continuous echoes" up to ~0835 LT. These continuous echoes occur not only during whole night and also during post-sunrise periods (Choudhary and Mahajan 1999; Ogawa et al. 2002). The echoes re-appeared around 0935 LT, around 60 minutes after the commencement of the eclipse. These echoes displayed discrete and nearly coherent patterns in RTI maps, which are similar to the "QP type" observed usually during the post-sunset period over low and mid latitudes. These QP type echoes lasted for around 45 minutes at around the 126 km range, with ~7 - 9 minute and ~3 - 5 minute periodicities. In addition, one additional region of echoes was also observed at higher altitude at around the 133 km range at 0938 LT, however only for a short while, and that was triggered in close coincidence with the peak time of the eclipse. Further, after a short gap (for about 20 minutes), a strong echo pattern was observed between 1040 and 1135 LT at around 130 km range and these echoes also showed QP type features. It should be noted that the large vertical extensions of these echoes were caused by range sidelobe which occurred primarily due to the fact that the Barker codes were employed to the transmitted pulses. It is worth mentioning here that the principle disadvantage of Barker codes is larger sidelobe response (Farley 1983). Interestingly, the Doppler velocities (middle panel in Fig. 3) of QP type echoes observed in both time

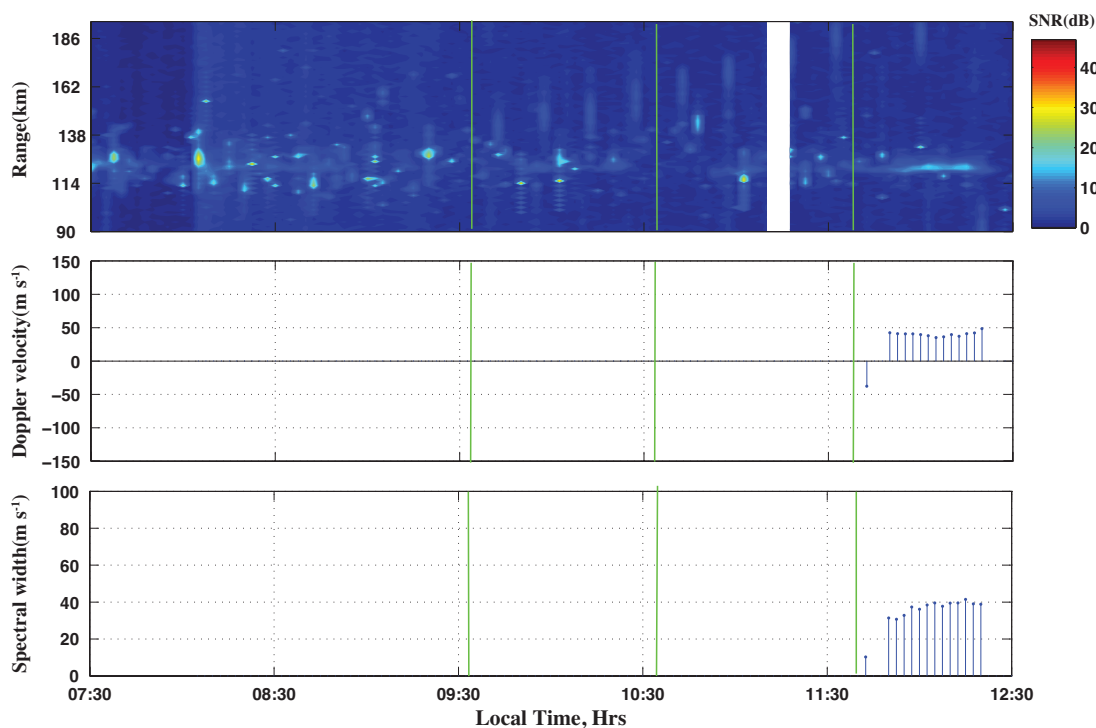


Fig. 2. Range-Time-Intensity map (top panel), Doppler Velocity (middle Panel), and spectral width plots (lower panel) obtained from the Chung-Li 52 MHz radar observations on 21 July 2009.

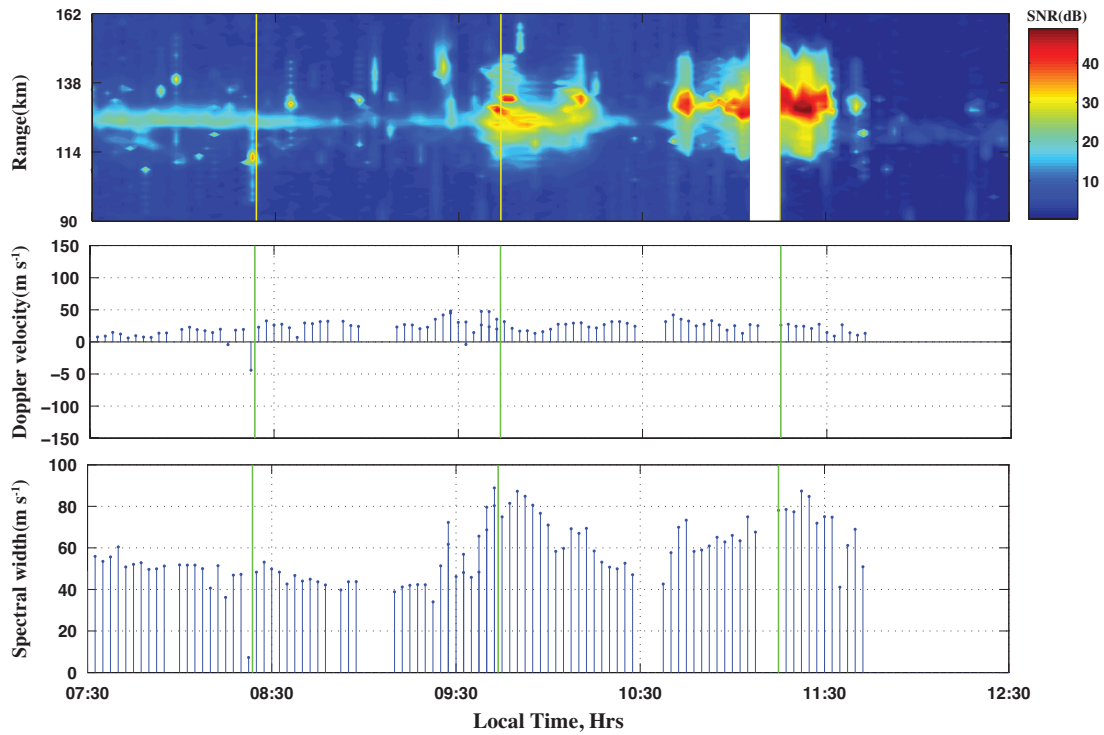


Fig. 3. Range-Time-Intensity map (top panel), Doppler Velocity (middle panel), and spectral width plots (lower panel) obtained from the Chung-Li 52 MHz radar observations on 22 July 2009.

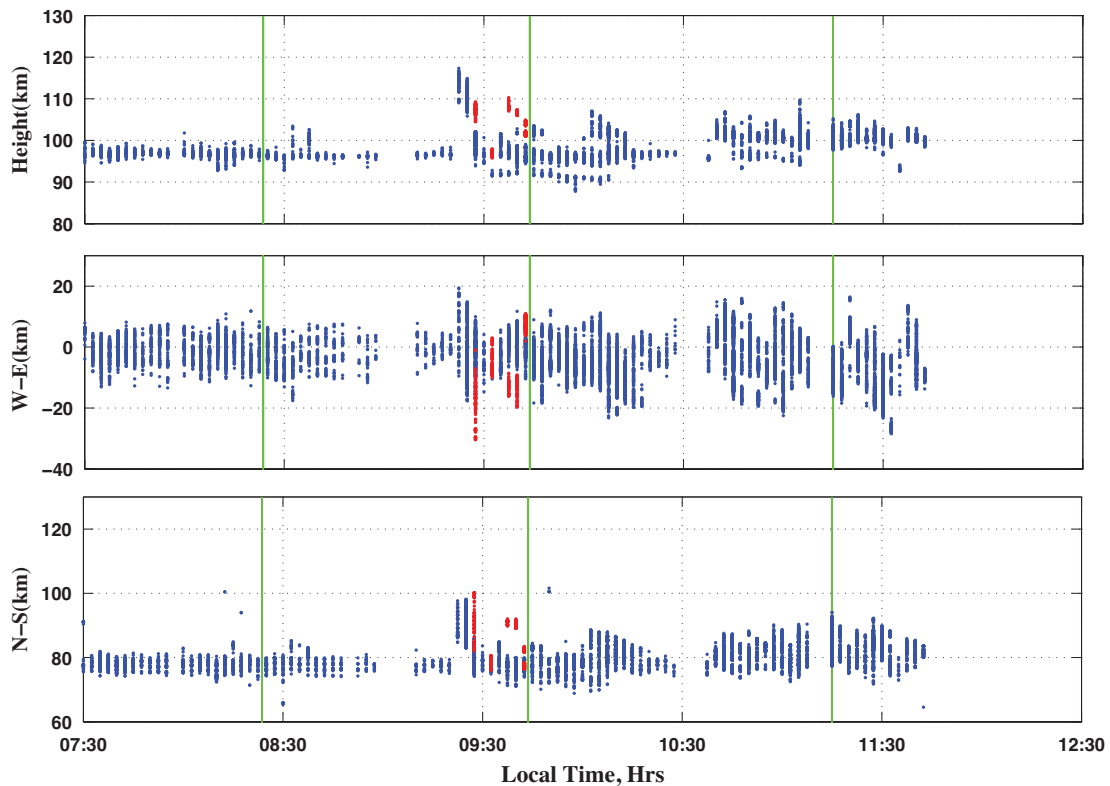


Fig. 4. Time sequences of the interferometer-resolved spatial distributions of Es echoes projected on the vertical (top panel) and horizontal (mid and bottom panels) planes. Note that the presence of short-lived additional layer is shown with red color lines.

Table 1. Radar specifications along with important parameters used for the experiment.

S. No.	Parameter	Values
1.	Location	Chung-Li (24.9°N, 121.2°E, Dip 35°N)
2.	Center frequency	52 MHz
3.	Peak transmitter power	120 kW
4.	Beam direction	17° West of geographic North
5.	Zenith angle	41°
6.	Receiving Channels	3
7.	Interpulse period	2.0 ms
8.	Pulse width	28 ms with 7 bits Barker code
9.	Coherent integration time	0.4 ms
10.	Range bins	60

slots showed a upward/northward direction with magnitudes around 45 - 50 m s⁻¹ and often have reached to greater than 55 m s⁻¹ when strong backscatter echoes were observed. Although echoes observed during pre-eclipse day are showing a upward/northward direction, only for less than 30 minutes, the Doppler velocities associated with these echoes have magnitudes of around 40 - 50 m s⁻¹. The upward/northward velocities during pre-eclipse, eclipse and post-eclipse on 22 July are consistent with what is normally expected from the daytime eastward electric field. The bottom panel in Fig. 3 depicts the corresponding spectral widths of continuous echoes which show relatively narrow widths (around 45 - 50 m s⁻¹), while the QP echoes which show between 60 and 80 m s⁻¹ and often reaching to magnitudes of 90 m s⁻¹ particularly during the incidents of strong backscatter echoes.

With interferometry measurements, three-dimensional spatial structures of the 3-meter FAIs in the echo region can be reconstructed (Chu and Wang 1997; Chu et al. 2011). Figure 4 shows the time sequence of echo patterns on 22 July 2009 projected on the vertical (top panel) and horizontal planes (middle and lower panels). Note that here we did not present the spatial components of echoes on 21 July 2009 as there were no significant echoes observed during that day. The spatial components on 22 July were obtained by operating the 52 MHz radar in interferometry mode by which the angular position and true height of the radar returns from Es irregularities in the echoing region could be determined unambiguously (Chu and Wang 1997). As can be seen from the Fig. 4, both continuous and QP echoes observed on 22 July 2009 were found to be located below 100 km, while QP echoes appeared between 1040 and 1135 LT were located above 100 km. Another important observation is that the significant appearance of an additional layer at around 107 - 108 km when maximum obscuration of the sun took place over the radar beam location and the presence of an addi-

tional layer is shown with red colored lines. It is important to mention here that the presence of a short-lived additional layer was also noticed during the peak time of eclipse in the ionogram and those observational results will be presented in later sections. The spatial distribution of echoes projected on a zonal plane, which was shown in the middle panel of Fig. 4, indicates clearly that the QP echoes were moving toward westerly direction with the progression of time. It is clear from these figures that both continuous and QP echoes were associated with different morphological features.

Figure 5 shows a typical ionogram recorded at 0945 LT on 22 July 2009. It is clear that an intensified range spread Es trace was present and the range spread Es trace is characterized by a relatively flat and sharp bottom edge and irregular top edges. Note that an intensified range spread Es trace witnessed between 0930 and 1025 LT and between 1040 and 1130 LT and the results are presented in the following section. Further, a clear look at the ionogram depicts an additional layer (shown with a black colored arrow symbol) is located at around the 123 - 124 km range. The multiple Es layers observed in the ionogram, therefore, bears a close resemblance with additional backscatter echoes observed using VHF radar at the peak time of the eclipse. In addition, the concurrent measurements of the 52 MHz radar backscatter and ionosonde range spread Es echoes strongly indicate that the electron density irregularities at various scale sizes from a meter to kilo-meter scale existed simultaneously in the Es layer in the same lines with the Chu et al. (2011) study.

Figure 6 shows the temporal variation of the top frequency of the reflecting/scattering of Es layer (ftEs) during 21 (red line), 22 (blue line), and 23 (black line) July 2009, in which initial, peak and final phases of the eclipse over Chung-Li radar location is shown with vertical arrow lines. It is very clear from this figure that a considerable increase in ftEs is evident on 22 July 2009 compared to other days

and that a considerable increase was found to be highest during peak time (around 21.9 MHz) followed by during the final phase (21.4 MHz) of solar eclipse. Further, a thorough examination of temporal variations of fEs during July 2009 has revealed that the top frequency of Es often varies between 9 - 12 MHz at around 0800 - 0900 LT, which clearly indicating the relatively strong Es activity (12.9 MHz) at around 0825 LT on 22 July 2009 belongs to mere day-to-day variability only. In addition, it can also be understood that the solar eclipse induced effects might not have worked by that too early time (~0820 - 0825 LT and ~0830 - 0845 LT on 22 July 2009) as the Chung-Li radar also did not record any strong back scatter echoes by that time. On the other hand, Fig. 7 depicts the temporal variation of the blanketing frequency of Es (fbEs) during 21, 22, and 23 July 2009. It is clear from this figure that fbEs was found to be present from 1130 LT onwards on 22 July 2009 with maximum values (6.6 MHz) between 1145 and 1155 LT, while fbEs on 23 July 2009 found to appear as patchy in character and it was completely absent on 21 July 2009.

3. DISCUSSION

At the outset, from relatively smaller Doppler velocities and broad spectral widths (middle and lower panels of Fig. 3), it can be concluded that the targets responsible for the Doppler spectra were type-2 plasma irregularities. It is generally believed that the mechanism involved in the generation of type-2 meter scale plasma irregularities in the Es layer is gradient drift instability through the non-linear cascade process (Fejer et al. 1984). According to the linear growth rate, Υ , of gradient drift instability, which has the following vector form (Woodman et al. 1991)

$$\Upsilon \propto \frac{1}{1 + \psi} \vec{k} \cdot \vec{V}_D (\vec{k} \cdot \Delta N \times \vec{B}) \quad (1)$$

where $\psi = \frac{\nu_e \nu_i}{\Omega_e \Omega_i} (1 + \frac{\Omega_e^2}{\nu_e^2} \sin^2 \phi)$

where k is the wavenumber of the plasma waves (or irregularities), ΔN is the vertical gradient of electron density, B is the magnetic field, and ν_i and ν_e are, respectively, the ion-neutral and electron-neutral collision frequencies, Ω_i and Ω_e are, respectively, the ion and electron gyro-frequencies, V_D is the relative electron-ion drift velocity that is driven by $E \times B$ drift effect, ϕ is magnetic aspect angle with respect to perpendicularity to the magnetic field line. Therefore, for the plasma irregularities of the Es layer, the excitation of the gradient drift instability requires an upward/northward pointed electric field and westward drift of the irregularities along with vertical plasma density gradients. The present observational results made with the 52 MHz radar have provided clear evidence of the presence of upward/northward pointed electric field (middle panel in Fig. 3) and westward

drift (middle panel in Fig. 4) and, it is therefore reasonable to conclude that the gradient-drift instability mechanism has been excited initially and then the meter-scale irregularities would have been generated from them through a non-linear turbulence cascade process (Farley 1985) so as to produce the backscatter echoes at 3-meter scale.

Having accounted for the observational evidence on upward/northward pointed electric fields, a natural question immediately arises that what are the plausible physical mechanisms responsible for the generation of these electric fields? It is generally thought that the neutral wind shear plays an essential role in the formation of the mid-latitude Es layer (Whitehead 1989). One of the most common and efficient ways to produce neutral wind shear in the Mesosphere and Lower Thermosphere (MLT) regions is the upward propagating tidal and gravity waves (Chu et al. 2011). According to Chimonas and Hines (1970) and Liu et al. (2011) as the lunar shadow boat sweeps at supersonic speed across the Earth, the cooling spot acts as a continuous source of gravity waves that build up into a bow wave. In this context, it turns out that there is sufficient observational evidence that points to the generation of gravity waves in the low latitude ionosphere during the 22 July 2009 solar eclipse (Chen et al. 2010; Liu et al. 2011). The presence of gravity waves is, therefore, pretty sure during this solar eclipse. Such wave activities would have been responsible for the sudden enhancement in Es activity (through wind shear mechanism) and the polarization electric fields in plasma structures of Es layer. It has been shown theoretically and experimentally that gravity wave-associated neutral wind may generate polarization electric field inside Es layer owing to differential collisions between neutral-ion and neutral-electron pairs (Gelinas et al. 2002; Chu et al. 2011). Chu et al. (2011) have shown schematically how polarization electric field could generate in an Es plasma structure by a gravity-wave induced neutral wind (Fig. 11 in their paper). According to Chu et al. (2011) a wave-induced polarization electric field will give rise to the drift of ions and electrons in the Es layer through the $E \times B$ effect. In order to fulfill the convergence requirement of the plasma for the Es layer formation in northern hemisphere, the wave-associated zonal neutral wind in the upper (lower) portion of the Es layer should be in the west (east) direction (Whitehead 1970). In the lower E-region below about 130 km, Hall conductivity is appreciably larger than Pedersen conductivity (Rishbeth and Garriott 1969). In that environment, because ion-neutral collision frequency is comparable to ion-gyrofrequency and electron-neutral collision frequency is much smaller than electron-gyrofrequency (Kelley 1989), one might expect that the westward (eastward) neutral wind will be responsible for eastward (westward) polarization electric field. In the presence of meter-scale FAIs, VHF coherent scatter radar will detect echoes from the upper (lower) Es layer which will have mean Doppler velocity away (toward) from the

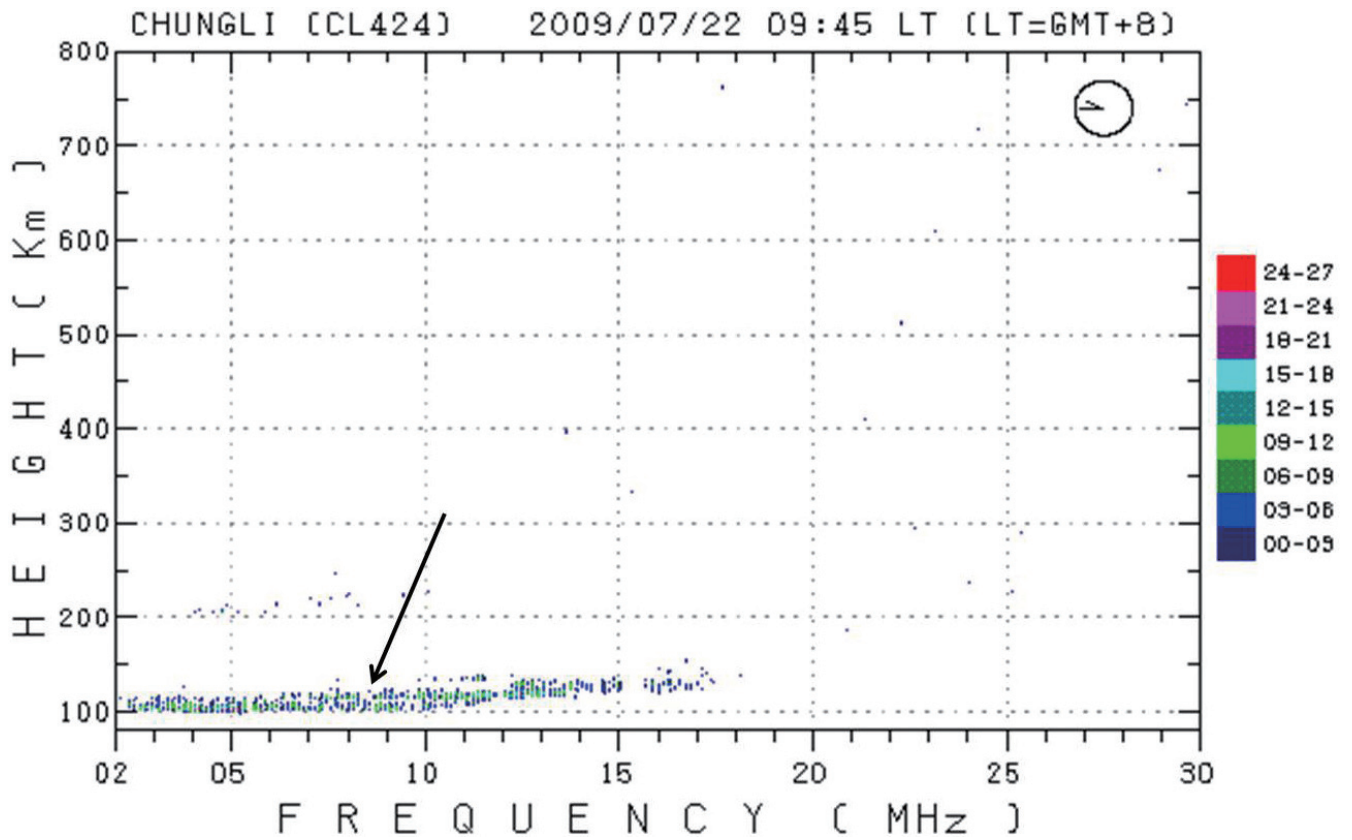


Fig. 5. Typical example of digital ionogram recorded at Chung-Li at 0945 LT on 22 July 2009. Note that the color code represents echo strength in unit dB.

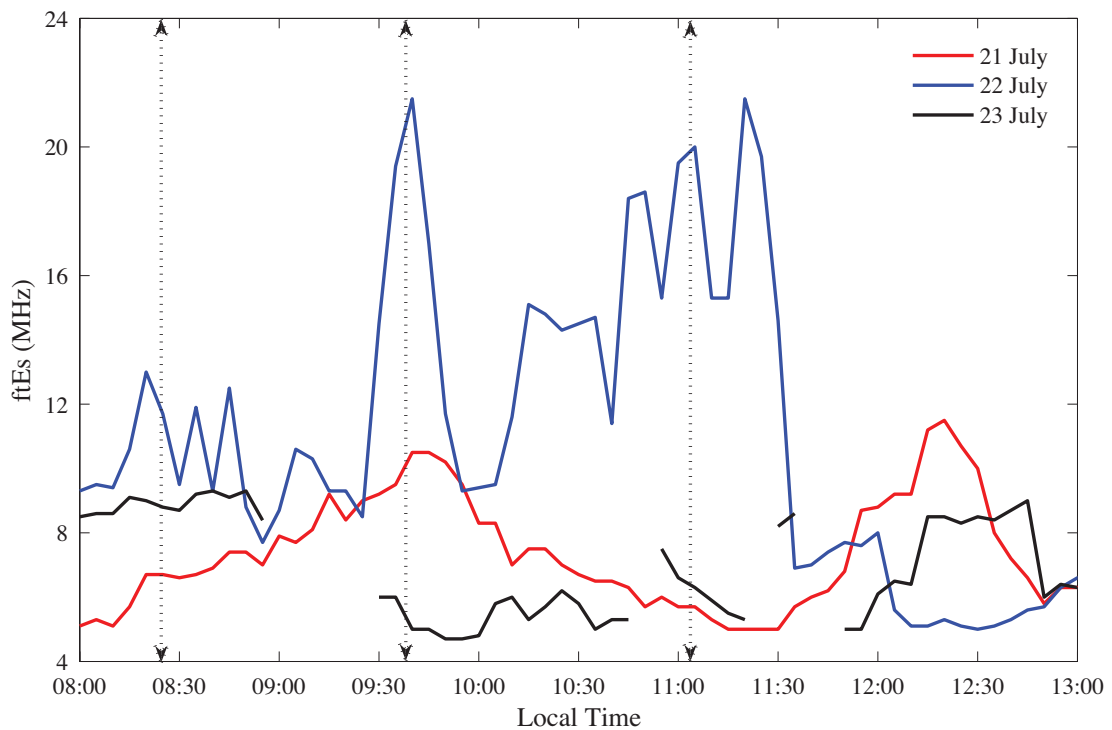


Fig. 6. Ionosonde observations of ftEs from Chung-Li during 21, 22 and 23 July 2009. Note that the initial, peak and final phases of solar eclipse over the Chung-Li radar location are shown with vertical arrow lines.

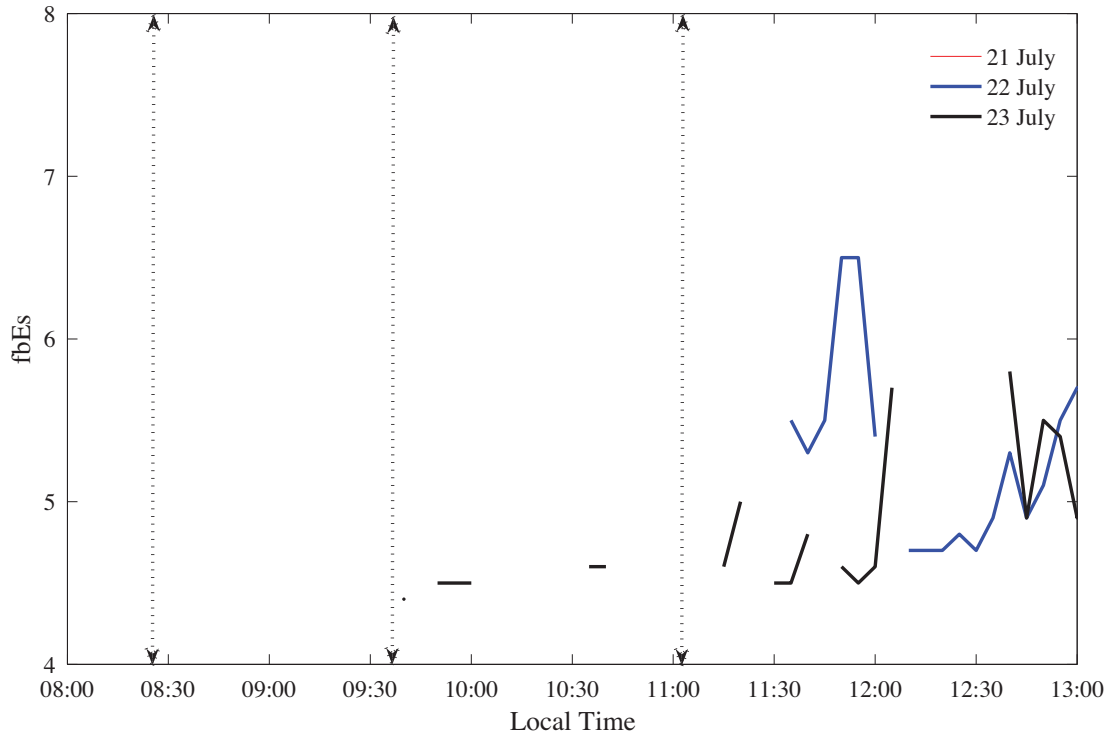


Fig. 7. Ionosonde observations of fbEs from Chung-Li on 21, 22 and 23 July 2009. Note that the initial, peak and final phases of solar eclipse over the Chung-Li radar location are shown with vertical arrow lines.

radar. Coincidentally, the observational results of the present study corroborate the notion proposed by Chu et al. (2011) (see the middle panel of Fig. 3). The induced polarization electric field by the neutral wind of the gravity wave with a short period Es layer has been studied by Gelinias et al. (2002) and according to Gelinias et al. (2002).

$$\Delta E_p = \frac{\lambda_{\parallel} \sigma_H B \Delta U}{\lambda_{\perp} \sqrt{\sigma_O \sigma_P} - \lambda_{\parallel} \sigma_P} \quad (2)$$

where ΔU and ΔE_p are, respectively, amplitudes of zonal wind velocity of the gravity wave and wave-induced polarization electric field, λ_{\parallel} and λ_{\perp} are, respectively, vertical and horizontal wavelength of the gravity wave, B is the magnetic field flux, σ_O , σ_P and σ_H are, respectively, parallel, Pedersen, and Hall conductivities. From Eq. (2), the relation between $E \times B$ drift velocity shear and the gravity wave-induced neutral wind shear can be written as follows:

$$\frac{\partial W}{\partial z} = \frac{\lambda_{\parallel} \sigma_H \partial U}{L_{\parallel} \sigma_P \partial z} \quad (3)$$

where $W (= \Delta E_p / B)$ is $E \times B$ drift velocity, $L_{\parallel} [= \lambda_T (\sigma_O / \sigma_P)^{\frac{1}{2}}]$ is the mapping distance of the electric field with zonal dimension λ_T along magnetic field line (Farley 1959). Note that the assumption of $(\sigma_O / \sigma_P)^{\frac{1}{2}} \gg 1$ has been made in de-

veloping Eq. (3), which is generally valid in Es region (Kelley 1989). According to Eq. (3) wherein the Doppler velocity shear ($\partial W / \partial z$) of FAIs is proportional to the neutral wind shear ($\partial U / \partial z$) that determines the plasma density in the Es layer formed through (wind) convergence process.

In order to verify the exact relation between the Doppler velocity shear and plasma densities, we present in Fig. 8 the spatial distributions of back scatter echoes (first panels), echo power (middle panels), and Doppler velocities (last panels) during the peak of this solar eclipse i.e., at 0935 LT (in Fig. 8a) and 0940 LT (in Fig. 8b) on 22 July 2009. As shown, a one-to-one correspondence between the peaks in Doppler velocity shear and the radar backscatter is found to be prevalent. In order to verify whether such correspondence is prevalent or not during other times, particularly between 1050 and 1130 LT, we have made a direct comparison between the Doppler velocity shear ($\partial W / \partial z$) and radar peak echo power. Figure 9 shows the direct comparison between Doppler velocity shear (red color solid line) and radar peak echo power (blue color solid line) between 0825 and 1150 LT on 22 July 2009. It is interesting to note that there is a great coherency between those two parameters during initial, peak and concluding phases of the solar eclipse which occurred on 22 July 2009 clearly indicating that the peak radar backscatter from the field-aligned irregularities of Es layer occurred at the node of the Doppler velocity shear.

It is also evident from Eq. (3) that the Doppler velocity

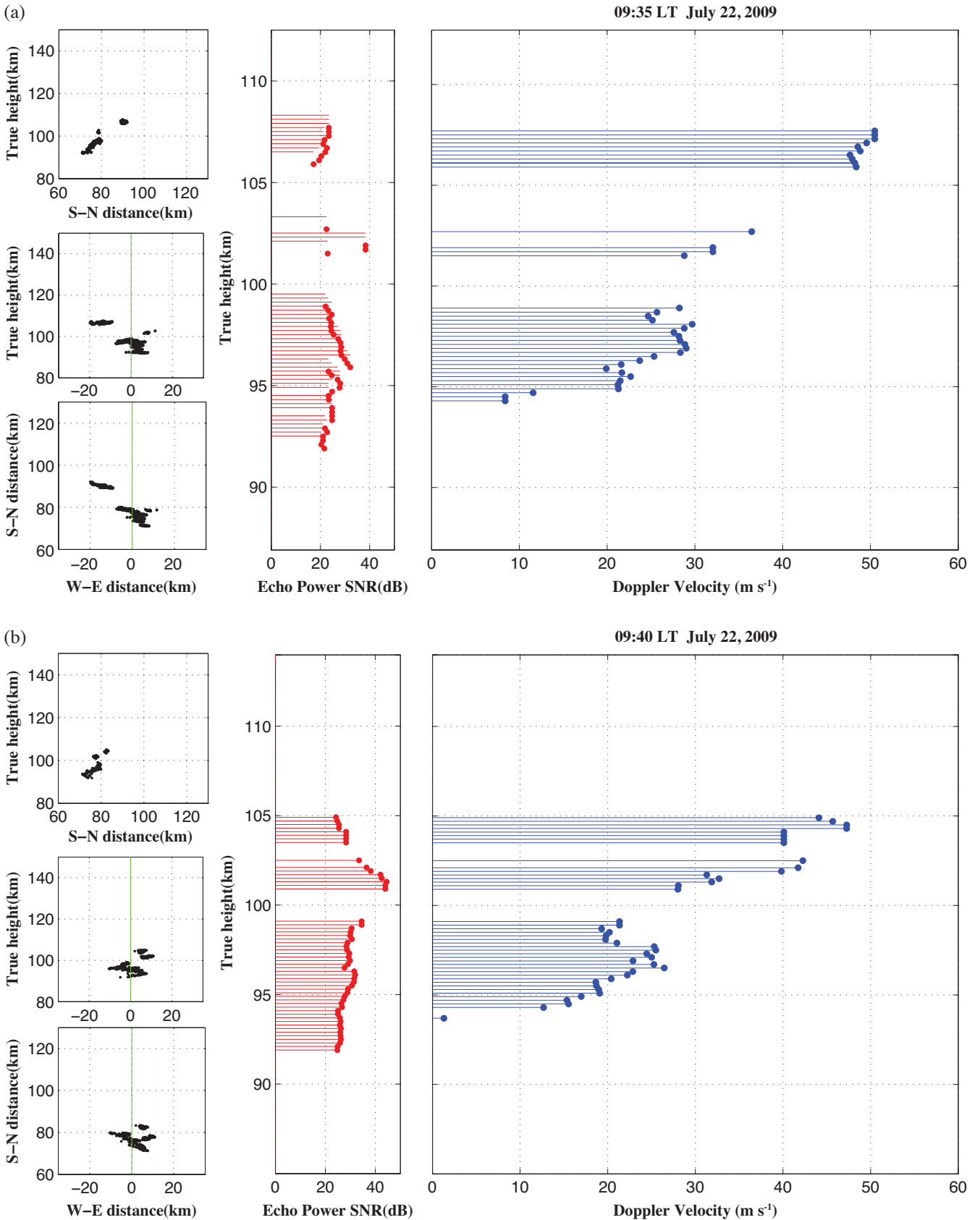


Fig. 8. Interferometer-resolved spatial distributions of Es echoes projected on different planes (both vertical and horizontal), echo power, and Doppler velocities measured using the Chung-Li radar during 0935 LT (a) and 0940 LT (b) on 22 July 2009.

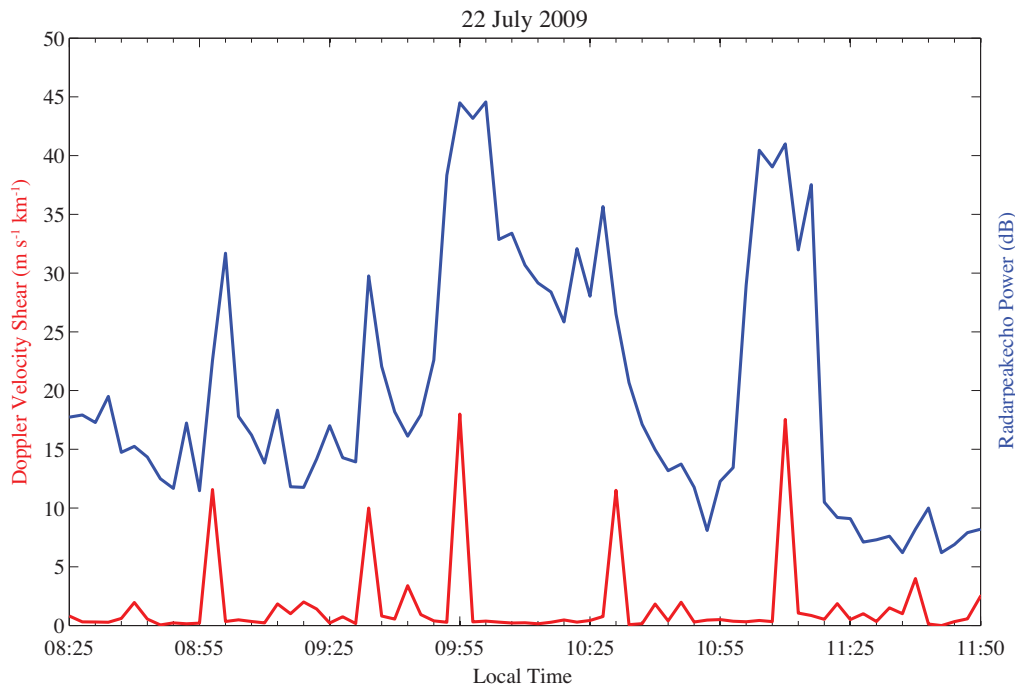


Fig. 9. Comparison between Doppler velocity shear ($\text{m s}^{-1} \text{km}^{-1}$) and radar peak echo power (dB) on 22 July 2009, wherein a one-to-one correspondence between them is clear.

shear is proportional to the vertical wavelength λ_r of the gravity wave. It follows from our observations that the gravity wave with vertical wavelengths of around 6 - 8 km could have existed during the peak time of this solar eclipse and that it could have helped in the formation of another layer at an altitude of ~ 107 km (see Figs. 3, 4 and 5 for about 6 - 8 km separation between the lower and upper Es layers). However, it is not possible to ascertain directly from this study at this time whether or not the solar eclipse could generate gravity waves with 6 - 8 km vertical wavelength.

4. SUMMARY AND CONCLUSION

The occurrence of a solar eclipse on 22 July 2009 enabled us to observe the ionospheric E-region irregularities over Chung-Li using the 52 MHz radar, for the first time during daytime. It is believed that these E-region irregularities were indeed induced by the eclipse effects. The significant observations during this rare natural event are: (1) appearance of QP type echoes along with an additional echo at higher altitudes with a short duration of time; (2) an abrupt intensification in the weak Es layer with an additional layer at higher range, and (3) the presence of vertical shears of the radar Doppler velocity in the Es layer that is believed to be caused by the upward propagating gravity waves and the peak radar backscatter echo at the node of the Doppler velocity shear.

Acknowledgements Dr. P. S. Brahmanandam (Anand), Postdoctoral Research Fellow, Institute of Space Science,

National Central University is supported by the National Science Council (NSC) of the Republic of China under the grants NSC-101-2811-M-008-012.

REFERENCES

- Chen, G., Z. Zhao, G. Yang, C. Zhou, M. Yao, T. Li, S. Huang, and N. Li, 2010: Enhancement and HF Doppler observations of sporadic-E during the solar eclipse of 22 July 2009. *J. Geophys. Res.*, **115**, A09325, doi: 10.1029/2010JA015530. [[Link](#)]
- Chimonas, G. and C. O. Hines, 1970: Atmospheric gravity waves induced by a solar eclipse. *J. Geophys. Res.*, **75**, 875, doi: 10.1029/JA075i004p00875. [[Link](#)]
- Choudhary, R. K. and K. K. Mahajan, 1999: Tropical E region field aligned irregularities: Simultaneous observations of continuous and quasiperiodic echoes. *J. Geophys. Res.*, **104**, 2613-2619, doi: 10.1029/1998JA900012. [[Link](#)]
- Chu, Y. H. and C. Y. Wang, 1997: Interferometry observations of three-dimensional spatial structures of sporadic E irregularities using the Chung-Li VHF radar. *Radio Sci.*, **32**, 817- 832, doi: 10.1029/96RS03578. [[Link](#)]
- Chu, Y. H., S. R. Kuo, C. Y. Wang, and H. C. Huang, 1996: Spectral behavior of VHF backscatter from ionospheric sporadic E irregularities in the equatorial anomaly crest zone. *Terr. Atmos. Ocean. Sci.*, **7**, 361-373.
- Chu, Y. H., P. S. Brahmanandam, C. Y. Wang, C. L. Su, and R. M. Kuong, 2011: Coordinated sporadic E layer

- observations made with Chung-Li 30 MHz radar, ionosonde and FORMOSAT-3/COSMIC satellites. *J. Atmos. Sol.-Terr. Phys.*, **73**, 883-894, doi: 10.1016/j.jastp.2010.10.004. [[Link](#)]
- Datta, R. N., 1972: Solar-eclipse effect on sporadic-E ionization. *J. Geophys. Res.*, **77**, 260-262, doi: 10.1029/JA077i001p00260. [[Link](#)]
- Davis, J. R., W. C. Headrick, and J. L. Ahearn, 1964: A HF backscatter study of solar eclipse effects upon the ionosphere. *J. Geophys. Res.*, **69**, 190-193, doi: 10.1029/JZ069i001p00190. [[Link](#)]
- Farley, D. T., 1959: A theory of electrostatic fields in a horizontally stratified ionosphere subject to a vertical magnetic field. *J. Geophys. Res.*, **64**, 1225-1233, doi: 10.1029/JZ064i009p01225. [[Link](#)]
- Farley, D. T., 1983: Pulse compression using binary phase codes. *Intern. Council Sci. Unions Middle Atmosphere Program*, **9**, 410-414.
- Farley, D. T., 1985: Theory of equatorial electrojet plasma waves: new developments and current status. *J. Atmos. Terr. Phys.*, **47**, 729-744, doi: 10.1016/0021-9169(85)90050-9. [[Link](#)]
- Fejer, B. G., J. Providakes, and D. T. Farley, 1984: Theory of plasma waves in the auroral E region. *J. Geophys. Res.*, **89**, 7487-7494, doi: 10.1029/JA089iA09p07487. [[Link](#)]
- Gelinas, L. J., M. C. Kelley, and M. F. Larsen, 2002: Large-scale E-region electric field structure due to gravity wave winds. *J. Atmos. Sol.-Terr. Phys.*, **64**, 1465-1469, doi: 10.1016/S1364-6826(02)00110-4. [[Link](#)]
- Hines, C. O., 1960: Internal atmospheric gravity waves at ionospheric heights. *Can. J. Phys.*, **38**, 1441-1481, doi: 10.1139/p60-150. [[Link](#)]
- Kelley, M. C., 1989: *The Earth's Ionosphere: Plasma Physics and Electrodynamics*, Academic Press, San Diego, California, 487 pp.
- Le, H., L. Liu, X. Yue, and W. Wan, 2008: The ionospheric responses to the 11 August 1999 solar eclipse: Observations and modeling. *Ann. Geophys.*, **26**, 107-116, doi: 10.5194/angeo-26-107-2008. [[Link](#)]
- Liu, J. Y., Y. Y. Sun, Y. Kakinami, C. H. Chen, C. H. Lin, and H. F. Tsai, 2011: Bow and stern waves triggered by the Moon's shadow boat. *Geophys. Res. Lett.*, **38**, L17109, doi: 10.1029/2011GL048805. [[Link](#)]
- Ogawa, T., O. Takahashi, Y. Otsuka, K. Nozaki, M. Yamamoto, and K. Kita, 2002: Simultaneous middle and upper atmosphere radar and ionospheric sounder observations of midlatitude E region irregularities and sporadic E layer. *J. Geophys. Res.*, **107**, 1275, doi: 10.1029/2001JA900176. [[Link](#)]
- Patra, A. K., S. Sripathi, V. Sivakumar, and P. B. Rao, 2004: Statistical characteristics of VHF radar observations of low latitude E-region field-aligned irregularities over Gadanki. *J. Atmos. Sol.-Terr. Phys.*, **66**, 1615-1626, doi: 10.1016/j.jastp.2004.07.032. [[Link](#)]
- Patra, A. K., S. Sripathi, P. B. Rao, and R. K. Choudhary, 2006: Gadanki radar observations of daytime E region echoes and structures extending down to 87 km. *Ann. Geophys.*, **24**, 1861-1869, doi: 10.5194/angeo-24-1861-2006. [[Link](#)]
- Patra, A. K., R. K. Choudhary, and J.-P. St.-Maurice, 2009: Solar eclipse-induced E-region plasma irregularities observed by the Gadanki radar. *Geophys. Res. Lett.*, **36**, L13105, doi: 10.1029/2009GL038669. [[Link](#)]
- Patra, A. K., P. Pavan Chaitanya, and D. Tiwari, 2011: Characteristics of 150 km echoes linked with solar eclipse and their implications to the echoing phenomenon. *J. Geophys. Res.*, **116**, A05319, doi: 10.1029/2010JA016258. [[Link](#)]
- Rishbeth, H. and O. K. Garriott, 1969: *Introduction to Ionospheric Physics*, Academic Press, San Diego, California.
- Sridharan, R., C. V. Devasia, N. Jyoti, D. Tiwari, K. S. Viswanathan, and K. S. V. Subbarao, 2002: Effects of solar eclipse on the electrodynamical processes of the equatorial ionosphere: A case study during 11 August 1999 dusk time total solar eclipse over India. *Ann. Geophys.*, **20**, 1977-1985, doi: 10.5194/angeo-20-1977-2002. [[Link](#)]
- Thampi, S. V., M. Yamamoto, H. Liu, S. Saito, Y. Otsuka, and A. K. Patra, 2010: Nighttime-like quasi periodic echoes induced by a partial solar eclipse. *Geophys. Res. Lett.*, **37**, L09107, doi: 10.1029/2010GL042855. [[Link](#)]
- Tsai, L. C. and J. Y. Liu, 1997: Ionospheric observations of the solar eclipse on Oct. 24, 1995 at Chung-Li. *Terr. Atmos. Ocean. Sci.*, **8**, 221-231.
- Van Zandt, T. E., R. B. Norton, and G. H. Stonehocker, 1960: Photochemical rates in the equatorial F₂ region from the 1958 eclipse. *J. Geophys. Res.*, **65**, 2003-2009, doi: 10.1029/JZ065i007p02003. [[Link](#)]
- Wang, C. Y. and Y. H. Chu, 2001: Interferometry investigations of blob-like sporadic E plasma irregularity using the Chung-Li VHF radar. *J. Atmos. Sol.-Terr. Phys.*, **63**, 123-133, doi: 10.1016/S1364-6826(00)00141-3. [[Link](#)]
- West, K. H., G. Goldsmith, D. Campbell, and S. Zandstra, 2008: Effects of the 16 February 1980 solar eclipse on the composition of the low-latitude ionosphere as seen by Atmosphere Explorer E. *J. Geophys. Res.*, **113**, A12308, doi: 10.1029/2007JA012997. [[Link](#)]
- Whitehead, J. D., 1970: Production and prediction of sporadic E. *Rev. Geophys.*, **8**, 65-144, doi: 10.1029/RG008i001p00065. [[Link](#)]
- Whitehead, J. D., 1989: Recent work on mid-latitude and equatorial sporadic-E. *J. Atmos. Terr. Phys.*, **51**, 401-424, doi: 10.1016/0021-9169(89)90122-0. [[Link](#)]
- Woodman, R. F., M. Yamamoto, and S. Fukao, 1991: Gravity wave modulation of gradient drift instabilities in mid-latitude sporadic E irregularities. *Geophys. Res. Lett.*, **18**, 1197-1200, doi: 10.1029/91GL01159. [[Link](#)]